Soil depth gradients in microbial growth kinetics under deeply- vs. shallow-rooted plants

Kyungjin Min[ab], Eric Slessarev[c], Megan Kan[c], Karis McFarlane[c], Erik Oerter[c], Jennifer Pett-Ridge[c], Erin Nuccio[c], Asmeret Asefaw Berhe[a]

[a] Department of Life and Environmental Sciences, University of California, Merced, CA 95343

[b] Center for Anthropocene Studies, Korea Advanced Institute of Science and Technology, Daejeon, South Korea 34141

[c] Physical and Life Sciences Directorate, Lawrence Livermore National Laboratory, Livermore, CA 94550

ABSTRACT

Climate-smart land management practices that replace shallow-rooted annual crop systems with deeply-rooted perennial plants can contribute to soil carbon sequestration. However, deep soil carbon accrual may be influenced by active microbial biomass and their capacity to assimilate fresh carbon at depth. Incorporating active microbial biomass, dormancy and growth in microbially-explicit models can improve our ability to predict soil's capacity to store carbon. But, so far, the microbial parameters that are needed for such modeling are poorly constrained, especially in deep soil layers. Here, we investigated whether a change in crop rooting depth affects microbial growth kinetics in deep soils compared to surface soils. We used a lab incubation experiment and growth kinetics model to estimate how microbial parameters vary along 240 cm of soil depth in profiles under shallow- (soy) and deeply-rooted plants (switchgrass) 11 years after plant cover conversion. We also assessed resource origin and availability (total organic carbon, ^{14}C, dissolved organic carbon, specific UV absorbance, total nitrogen, total dissolved nitrogen) along the soil profiles to examine associations between soil chemical and biological parameters. Even though root biomass was higher and rooting depth was deeper under switchgrass than soy, resource availability and microbial growth parameters were generally similar between vegetation types. Instead, depth significantly influenced soil chemical and biological parameters. For example, resource availability, and total and relative active microbial biomass decreased with soil depth. Decreases in the relative active microbial biomass coincided with increased lag time (response time to external carbon inputs) along the soil profiles. Even at a depth of 210-240 cm, microbial communities were activated to grow by added resources within a day. Maximum specific growth rate decreased to a depth of 90 cm and then remained consistent in deeper layers. Our findings show that > 10 years of vegetation and rooting depth changes may not be long enough to alter microbial growth parameters, and suggest that at least a portion of the microbial community in deep soils can

grow rapidly in response to added resources. Our study determined microbial growth parameters that can be used in microbially-explicit models to simulate carbon dynamics in deep soil layers.

KEYWORD:

deep soil, microbial growth, active biomass, switchgrass, resource availability, microbial dormancy, ^{14}C, dissolved organic carbon

INTRODUCTION

Soil contains the largest carbon (C) pool in terrestrial ecosystems (IPCC, 2013; Jobbágy and Jackson, 2000). Accrual of organic C along soil depth gradients can contribute to climate change mitigation through sequestration of atmospheric carbon dioxide (Paustian et al., 2016). However, most soil C dynamics research so far has focused on the top 30 cm of soil, where soil C concentrations are highest (Jobbágy and Jackson, 2000; Kögel-Knabner et al., 2008). Recent studies highlight that surface soil (< 30 cm) and deep soil (> 30 cm) C pools respond differently to changes in environmental conditions (Berhe et al., 2008; Fierer et al., 2003a; Jia et al., 2019; Min et al., 2020; Pries et al., 2017). At the surface, variation in abiotic factors such as temperature and moisture can influence microbial transformation of soil organic C. However, in deeper soil layers, relatively constant environmental conditions, increased mineral interactions, and lower microbial biomass, combined with distinct microbial community composition, may alter the capacity for microbial C transformation relative to the surface (Rumpel et al., 2012; Rumpel and Kögel-Knabner, 2011). Given that most soil C is stored in deep soils (Jobbágy and Jackson, 2000) , we must establish a better understanding of how microbially-driven C dynamics vary along soil depth gradients.

Microorganisms modify the amount and chemical composition of soil organic matter via decomposition, respiration, growth, and death. Due to the critical roles microbes play in soil C dynamics, several biogeochemical models have recently incorporated microbial parameters (Allison et al., 2010; Salazar-Villegas et al., 2016; Wang et al., 2015; Wieder et al., 2015, 2013). Active microbial biomass and microbial growth rates are both key parameters in microbially-explicit models (He et al., 2015; Zha and Zhuang, 2020), but are poorly quantified because of the technical difficulty of direct quantification (Geyer et al., 2016). Most empirical measurements of microbial biomass reflect total biomass, using

62 analyses made with chloroform fumigation (Anderson and Domsch, 1978; Vance et al., 1987),
63 phospholipid fatty acid (Kao-kniffin and Balser, 2008; Kohl et al., 2015) or ATP (Contin et al., 2001;
64 Martens, 1995) approaches. However, since total microbial biomass comprises both active and dormant
65 biomass, and active microbial biomass is more relevant to biogeochemical cycles (Couradeau et al.,
66 2019; Geyer et al., 2016; Salazar-Villegas et al., 2016; Singer et al., 2017), using total microbial biomass
67 in models may be inadequate when projecting soil C dynamics. Microbial growth and dormancy can be
68 estimated from growth kinetics models (Mitchell et al., 2004; Panikov and Sizova, 1996), as well as
69 quantitative stable isotope probing (Koch et al., 2018; Pett-Ridge and Firestone, 2017; Schwartz et al.,
70 2016), nucleotide analog tagging (Allison et al., 2008; Hanson et al., 2008), and amino acid-tagging
71 approaches (Couradeau et al., 2019; Hatzenpichler et al., 2014).
72
73 In 1995, Panikov (1995) developed a model that parses microbial respiration sources into growth vs.
74 non-growth related respiration and estimates growth-related parameters (e.g., active vs. dormant
75 microbial biomass, the lag phase before exponential growth, and maximum specific growth rate; See
76 Methods). This approach is useful because it requires readily measurable microbial respiration as an
77 input, and the estimated microbial parameters can be directly used in microbially-explicit models. Using
78 the Panikov model, Blagodatskaya et al. (2014) demonstrated that rhizosphere microbes exhibit a
79 shorter lag time than non-rhizosphere microbes, due to their higher proportion of active biomass and
80 associated lower dormancy. Also, Salazar-Villegas et al. (2016) demonstrated that neither warming nor
81 wetting treatments alter maximum specific growth rates of soil microbial communities.
82
83 Changes in resource availability with soil depth may influence microbial growth parameters. The
84 amounts of organic C, nitrogen (N), and other resources are often higher at the soil surface where inputs
85 from plant litter and root exudates are concentrated (Jobbágy et al., 2001; Rumpel and Kögel-Knabner,

2011). In contrast, deeper layers receive limited direct plant inputs; typically, only dissolved organic matter that moves downward through mass flow or diffusion. In addition, mineral-organic matter associations in deeper layers can reduce microbial access to resources (Schmidt et al., 2011). Some studies suggest that soil microorganisms grow faster when resources are more abundant. For example, Blagodatskaya et al. (2010) demonstrated that more C inputs into soils under elevated CO_2 increased microbial maximum specific growth rate.

Similarly, rhizosphere microbes exhibited greater maximum specific growth rates and shorter lag times than bulk soil microbes (Blagodatskaya et al., 2014). Recent research suggests that these rapid growth responses to resource additions may be driven by traits related to microbial evolutionary history, taxonomy, 16S rRNA gene copy number or genome size (Li et al., 2019; Morrissey et al., 2019). Given the expected decreases in resource availability along soil depth profiles, it is plausible that microbial dormancy increases and the capacity for a rapid growth response declines with soil depth. It is also possible that microbial lag time increases with soil depth because microbes in deeper layers may be more likely to use strategies such as sporulation, and some of the abundant taxa in deep soils have been shown to decrease in relative abundance after soil fertilization (Brewer et al., 2019). Yet, it is unclear how the direction and magnitude of microbial growth parameters vary with soil depth profiles.

Improved understanding of depth-specific microbial growth kinetics is key for climate-smart land management practices that consider implementation of improved root phenotypes and/or replacement of annual crops with deeply rooted perennials (Paustian et al., 2016). One model deeply rooted species that is being considered in these efforts is switchgrass, a perennial grass native to North America, with a deep rooting system that extends up to 3 m (Liebig et al., 2005; Wright, 2007). Conversion from annual crops to switchgrass can significantly increase deep soil C stocks (Slessarev et al., 2020b). Deeply rooted

plant contributions to increased soil C storage are likely tied to changes in the distribution of rhizodeposits, water flow through the soil profile, and the types of microbial communities that thrive in the rhizosphere. For example, in switchgrass fields, enhanced production of extracellular polymeric substances and higher soil aggregate formation have been measured relative to annual crops (Sher et al., 2020), and linked to increased soil C storage with depth (Blanco-Canqui et al., 2005; McGowan et al., 2019; Sher et al., 2020). Also, switchgrass roots increased microbial OTU (operational taxonomic unit) richness along 60 cm of the soil profile (He et al., 2017). To our knowledge, no data currently exists on how the conversion of an annual crop to a deep-rooted perennial crop, such as switchgrass, impacts microbial growth and growth-related parameters (e.g., dormancy, active biomass) in deeper soil layers.

Here, we investigate microbial growth parameters along soil depth profiles under deeply- (switchgrass) and shallow-(soy) rooted plants. We collected soils under switchgrass and soy plots (n=3, each) from adjacent, paired field locations at soil sampling depths ranging from 0 to 240 cm. We incubated these soils with yeast extract as an added C and energy source, and monitored CO_2 efflux to parameterize a growth kinetics model according to a previously described approach (Blagodatsky et al., 2006; Wutzler et al., 2012). By fitting a growth kinetics model to the CO_2 data, we estimated total and active microbial biomass, maximum specific growth rate, and lag time. In addition, we quantified resource availability prior to the yeast extract addition to explore the interaction of depth and resource availability on microbial parameters. We hypothesized that (1) increasing depth would decrease maximum specific growth rate, due to decreasing resource availability (available C, N), (2) active biomass would be highest in surface soil layers while lag time would be greatest in deep soil layers, due to reductions in resource availability, and (3) microbial growth parameters would be less affected by depth under switchgrass than soy, because greater rooting depth results in more abundant resources inputs at depth.

METHODS

Study site and soil sampling

The study site is located near Bristol, South Dakota (45°16'N, 97°50'W), where switchgrass (*Panicum virgatum* L.; cultivar, Sunburst) has been growing since 2008 (Sekaran et al., 2019). Before switchgrass was cultivated, the site was used for soy. The mean annual temperature is 6.3°C, mean annual rainfall is 638 mm, and mean annual snowfall is 1092 mm at the nearest weather station in Webster, South Dakota (~32 km away, https://www.usclimatedata.com/climate/webster/south-dakota/united-states/ussd0368/2018/1). The study site is part of a long-term nitrogen (N) addition experiment (0, 56, and 112 kg urea-N ha^{-1} yr^{-1} since 2008), however, only control sites (0 kg N) were used for this experiment. The soils are classified as Fine-loamy, mixed, superactive, frigid Calcic Hapludolls (Barnes series, USDA Soil Taxonomy) and Fine-loamy, mixed, superactive, frigid Typic Calciudolls (Buse series, USDA Soil Taxonomy). The parent material is glacial till dominated by fine-grained sedimentary rocks deposited in the upper Pleistocene (Mankato substage, approximately 14 ka before present (Flint, 1955)). Each treatment plot is 21.3 m x 365.8 m with a 2-20% slope.

In July 2019, we collected a 240 cm deep soil core under switchgrass from each of three non-fertilized plots on a crest landscape position (n=3) using a Geoprobe® 54LT direct push machine (Salina, Kansas, USA) combined with a MC7 system (diameter: 7.62 cm). For comparison, we also collected three 240 cm of deep soil cores in a soy field adjacent to the switchgrass plots (n=3). Since 2008, this field has been primarily used to grow soy and intermittently cropped with other annuals (spring wheat or corn or maintained as pasture (USDA NASS 2020; https://nassgeodata.gmu.edu/CropScape/)). After extraction, soil cores were immediately divided into nine sections using a hybrid fixed depth and soil horizon method, i.e., when there was a clear separation between soil horizons by color or texture, we divided

157 sections using a generic horizon approach. Otherwise, we divided soil cores into 20 cm increments for
158 the top 60 cm soil and 30 cm increments for depths below 60 cm. Hereafter, we refer to the soil depth
159 sections as 0-20, 20-40, 40-60, 60-90, 90-120, 120-150, 150-180, 180-210, and 210-240 cm for simplicity
160 of visual representation. After soil cores were subsectioned, we removed rocks and roots manually in
161 the field, shipped the samples to the University of California-Merced in a cooler, and stored them at 4°C.
162 Within a week of arrival, soil samples were processed to determine soil physical, chemical, and microbial
163 properties. In the lab, more roots were hand-picked if necessary. Roots collected from soil cores were
164 dried and weighed to quantify root distribution along soil depth profiles.

165

166 Soil physicochemical properties

167 Soil pH was determined in water (1:5, fresh soil weight:water volume) using a Mettler Toledo pH meter.
168 We extracted dissolved organic C (DOC) by mixing 6 g of fresh soil with 30 mL of 0.5 M K_2SO_4 and shaking
169 the soil solution for 4 h. The soil solution was then centrifugated at 2,000 rpm for 5 min and the
170 supernatant was filtered through a 0.45 μm membrane filter (PALL, Port Washington, NY, USA). The
171 filtrate was stored at -20°C until analysis. The DOC concentration and dissolved N in K_2SO_4 extracts were
172 determined using a VCSH Total OC Analyzer (SHIMADZU, Kyoto, Japan) after thawing in the
173 Environmental Analytical Lab at the University of California-Merced. To estimate the easiness of
174 microbial utilization, we quantified Specific UV Absorbance at 254 nm (SUVA) on K_2SO_4 extracts, using a
175 UV-VIS spectrophotometer (Evolution 300, Thermo Scientific, Massachusetts, USA). Higher SUVA values
176 indicate a higher relative abundance of aromatic compounds in DOC extracts (Weishaar et al., 2003) and
177 less available form of DOC to microbes.

178 Total C and N were quantified on dried and ground soils at the Oregon State University Crop and Soil
179 Science Central Analytical laboratory. Because soils in both vegetation types were alkaline with pH

between 8.0 and 9.3 (S1), we treated soils with 1M HCl to remove carbonates before determining total OC concentrations. Inorganic C was quantified at Lawrence Livermore National Laboratory by treating finely-ground subsamples of each sample with 1 M phosphoric acid in a sealed jar and measuring CO_2 evolved using a LI-850 infrared gas analyzer (Robertson et al., 1999) for 24 h. Total OC and ^{13}C were quantified on acid-treated soils (treatment with 1 M HCl) at the Integrative Biology Center for Stable Isotope Biogeochemistry Lab at the University of California-Berkeley.

We assessed radiocarbon values on soils from 0 cm to 150 cm only. Radiocarbon values were measured on the NEC 1.0 MV Tandem Accelerator Mass Spectrometer (AMS) or the FN Tandem Van de Graaff AMS at the Center for Accelerator Mass Spectrometry (CAMS) at Lawrence Livermore National Laboratory. Prior to measurement, acid-treated soils were prepared for ^{14}C measurement by sealed-tube combustion to CO_2 in the presence of Ag and CuO and reduced onto Fe powder in the presence of H_2 (Vogel et al., 1984). The ^{14}C content of each sample was reported in $\Delta^{14}C$ notation, corrected for mass-dependent fractionation with measured $\delta^{13}C$ values, and then corrected to the year of measurement for ^{14}C decay since 1950 (Stuiver and Polach, 1977).

Soil incubation and CO_2 measurement

For soil incubations, 20 g of fresh soil was weighed into a polypropylene incubation jar (McMaster-Carr, 473 mL) and pre-incubated at 22°C overnight (108 jars = 2 vegetation types * 9 depths * 3 replicate cores * 2 amendment treatments). For treatment jars, we added 40 mg of powder yeast extract g^{-1} dry soil as a C and nutrient source (VWR). We chose yeast extract over glucose to provide more varied forms of C and thus stimulate more diverse microorganisms (Fierer et al., 2003b; Slessarev et al., 2020a). A preliminary experiment confirmed that the amount of yeast extract added to the soil was enough to avoid limiting growth during ~10 h of exponential growth phase. After the yeast extract was added, we

adjusted the soil water content to 60% of water holding capacity (initial gravimetric water content was 18.6 ± 3.7%) and stirred the soils for 30 s. For control jars, only water was added to soils without yeast extract. The jars were closed with a lid equipped with a non-dispersive infrared CO_2 sensor (CM0126-FS, 1% CO_2 sensor, CO_2 meter) (Harmon et al., 2015). We monitored CO_2 concentrations for 10 min every 30 to 60 min during the incubation (24~30 h), computed the slope of CO_2 concentration over time, and quantified the microbial respiration rate (μg C-CO_2 g^{-1} dry soil h^{-1}).

Microbial growth kinetics

We measured microbial growth kinetics using the Panikov model approach, which makes three assumptions (Panikov, 1995; Panikov and Sizova, 1996): First, microbes are not limited by resources (C, water, and nutrients) during incubation. Second, microbial parameters that are estimated from the model refer to those for the initial microbial community, not for the final microbial community after the activation by resources. Three, microbial parameters estimated from the model refer to those from a whole microbial community, undifferentiated among microbial taxa. Under such conditions, microbial respiration follows the equation:

$$v\,(t) = A + B \cdot \exp(\mu_{max} \cdot t)$$

Where v is total microbial respiration rate (μg C-CO_2 g^{-1} dry soil h^{-1}) at time t, A is non-growth respiration of the initial microbial community (μg C-CO_2 g^{-1} dry soil h^{-1}), B is growth-based respiration of the initial microbial community (μg C-CO_2 g^{-1} dry soil h^{-1}), μ_{max} is the maximum specific growth rate of the initial microbial community (h^{-1}), and t is the time elapsed since the C and nutrients addition (h). Fitting of this growth kinetics model to our CO_2 data was restricted to the initial exponential growth phase (inflection point) to accurately capture unlimited growth and maximize the goodness of fit r^2 (Wutzler et al., 2012).

Physiological status of the initial microbial biomass (relative active biomass) was calculated as below.

226 $$r_0 = \frac{B\ (1-\lambda)}{A + B(1-\lambda)}$$

227 Where r_o is relative active biomass of the initial microbial community (unitless) and λ is the ratio of
228 maximum specific rate of growth-related substrate uptake over maximum specific rate of total substrate
229 uptake under unlimited growth. Trutko et al. (1984) demonstrated that the value of λ varied between
230 0.8-0.9 over 100 microbial species. As previous studies exploring microbial growth kinetics have
231 employed λ=0.9 (Blagodatskaya et al., 2014; Blagodatsky et al., 2006; Panikov and Sizova, 1996), we
232 also used 0.9 for this study. The value of r_o varies between 0 and 1, with 0 when all microbes are
233 dormant and 1 when all microbes actively grow and divide cells.

234 Total initial microbial biomass was calculated as per the following:

235 $$x_0 = \frac{B \cdot \lambda \cdot Y_{CO2}}{r_0 \cdot \mu_{max}}$$

236 Where x_o is the total initial microbial biomass (μg C-biomass g^{-1} dry soil), and Y_{CO2} is biomass yield per
237 unit CO_2 respired. We acknowledge that Y_{CO2} can vary with changes in environmental conditions such as
238 temperature and C availability (Lehmeier et al., 2016; Manzoni et al., 2012; Min et al., 2016). However,
239 during the experiment, microbes were allowed to grow under unlimited C and at a constant
240 temperature of 22°C. Thus, we assumed that Y_{CO2} is constant at 1.5, which corresponds to a commonly
241 observed microbial C use efficiency of 0.6 (Keiblinger et al., 2010; Manzoni et al., 2012; Min et al., 2016).

242 We define lag phase (t_{lag}) as the period when non-growth respiration is equal to or less than growth-
243 related respiration.

244 $$A = B \cdot \exp(\mu_{max} \cdot t_{lag})$$

245 $$t_{lag} = \frac{\ln(\frac{A}{B})}{\mu_{max}}$$

246

247 We assume the longer the lag time is, the higher degree of microbial dormancy. Details about the
248 derivatization and calculation of these growth kinetics equations are provided in previous studies
249 (Blagodatsky et al., 2006; Panikov, 1995; Panikov and Sizova, 1996).

250

251 Statistics

252 Data are presented as mean ± standard error, where n = 3 from replicate cores across soil depth profiles
253 and vegetation types. We fit the Panikov model to the microbial respiration data and estimated
254 microbial growth parameters using a nonlinear least-squares approach (*nls* function in R, R Core Team
255 3.6.3). The effects of vegetation and depth on microbial growth parameters, resource availability, and
256 root biomass were tested using a linear mixed-effects model, with vegetation and depth as explanatory
257 variables and soil core as a random variable (nlme package, *lme* (linear mixed effects) function,
258 restricted maximum likelihood method). Depth was treated as continuous. When there was a significant
259 interaction of vegetation type and depth, we used Tukey *posthoc* tests to compare soy and switchgrass
260 values at each depth (multcomp package, *glht* (general linear hypotheses) function, Tukey method). All
261 significance was tested at $\alpha = 0.05$.

262

RESULTS

Depth profiles of root biomass and resource availability

Increasing depth decreased root biomass for both vegetation types (p = 0.002; Fig. 1). No root was detected below 60 cm under soy, while we found roots under switchgrass till 150-180 cm. At a given depth interval, switchgrass produced more roots than soy along soil depth profiles (p = 0.004; Fig.1).

Overall, resource availability declined with soil depth but did not differ between vegetation types (Fig. 2). For example, total OC was highest at 0-20 cm for both vegetation types, decreased between 0-20 cm and 40-60 cm, then kept similar below (Fig. 2a). We observed greater total OC concentrations under soy than switchgrass at 0-20 cm. Soil depth decreased ^{14}C values, but vegetation types had little influence on the ^{14}C values (Fig. 2b). Below 90 cm, ^{14}C values approached -1000 per mille, which suggests a mean OC age greater than the geologic substrate's age (Upper Pleistocene ~ 14 ka (Martin et al., 2004)). This likely reflects contributions of fossil OC from the Pierre Shale, a major constituent of glacial till in eastern South Dakota (Flint, 1955), and the underlying bedrock in the region (Tomhave and Schulz, 2004) with an OC content up to several percent (Gautier, 1986; Kennedy et al., 2002).

DOC significantly decreased with depth and did not vary between vegetation types (Fig. 2c). At 0-20 cm, the average DOC concentration across vegetation types was 113.2 μg g^{-1}, twice that at 20-40 cm (p < 0.001). Below 60 cm, the DOC concentration was relatively similar across depths. Depth, but not vegetation type, significantly influenced aromaticity of DOC, measured as SUVA (Fig. 2d).

Both total N and dissolved N were significantly influenced by the interaction of depth and vegetation (p < 0.001 and 0.012, respectively; Fig. 2e,f). At 20-40 cm and 40-60 cm, total N content was higher under

soy than under switchgrass (p = 0.03 and 0.07, respectively). In contrast, dissolved N was similar between soy and switchgrass at 0-20 cm, but was significantly higher under soy at depths below 20 cm.

Microbial respiration

Basal respiration, before adding yeast extract, was similar across vegetation and depth (S2). When the data was pooled, the average rate of basal respiration was 0.45 ± 0.02 μg C-CO_2 g^{-1} dry soil h^{-1}. We observed distinct patterns in microbial respiration after the addition of water (control) versus water plus yeast extract (treatment) to soils (Fig. 3). Water addition did not alter microbial respiration (Fig. 3a), whereas water plus yeast extract immediately enhanced microbial respiration more than ten times (Fig. 3b). Then, in the following 30 hours, the yeast extract treatment's respiration rate became relatively stable, increased exponentially, then dropped when all the available resources were consumed.

Growth parameters

We fit the Panikov model to the microbial respiration data to compare microbial growth parameters across depth and vegetation (Fig. 4). Similar to the patterns in resource availability across vegetation and soil depth, we observed a significant depth effect on microbial parameters (except for maximum specific growth rate), but vegetation had little effect on microbial growth kinetics (Fig. 5).

Total microbial biomass was significantly influenced by depth, but not by vegetation or vegetation and depth interaction (Fig. 5a). When we pooled the data across vegetation, total microbial biomass was 131.8 ± 9.6 μg C g^{-1} dry soil at 0-20 cm and decreased by 77% to 30.5 ± 3.0 μg C g^{-1} dry soil at 210-240 cm.

309 Overall, the relative active biomass decreased along soil depth profiles, with a 143 times of reduction
310 from the surface to a depth of 210-240 cm (Fig. 5b). We found that at 40-60 cm, where there was no
311 difference in the total microbial biomass between soy and switchgrass (Fig. 5a), the relative active
312 biomass was two times greater under soy than under switchgrass (p = 0.04; Fig. 5b).
313
314 Lag time increased with soil depth profiles (Fig. 5c) and decreased with relative active biomass (S3). The
315 interaction of depth and vegetation significantly influenced lag time (Fig. 5c). At 40-60 cm, the average
316 lag time under soy was 6.1 h, 27% faster than microbes under switchgrass (p = 0.024). At 0-20 cm, the
317 lag time was marginally shorter for microbes under switchgrass than those under soy (p = 0.07). We
318 observed that microbes at 210-240 cm were activated to grow within 20 h after the yeast extract
319 additions (Fig. 5c).
320
321 Even though the maximum specific growth rate (μ_{max}) declined between 0 cm and 90 cm (p = 0.011),
322 when we included all depths between 0-240 cm, the depth effect was not significant (p =0.234). The
323 average value of maximum specific growth rate was 0.33 ± 0.01 h^{-1} across depth and vegetation (Fig.
324 5d). The maximum specific growth rate was independent of microbial biomass, regardless of whether
325 we compared it to total microbial biomass (Pearson's correlation coefficient r = -0.41, R^2< 0.001, p=0.01)
326 or relative active biomass (Pearson's correlation coefficient r = -0.18, R^2= 0.004, p=0.28).
327
328 Except for maximum specific growth rate, microbial growth parameters had a strong relationship with
329 total OC, DOC, total N, and dissolved N (Table 1). Resource availability was positively related to total and
330 relative active biomass, and negatively related to lag time. The μ_{max} values had no relationship with any
331 soil chemistry index tested in this study.

DISCUSSION

Active microbial biomass drives biogeochemical processes (Couradeau et al., 2019; Geyer et al., 2016; Graham et al., 2016; Salazar-Villegas et al., 2016; Singer et al., 2017; Wutzler et al., 2012), but is hard to characterize due to the inefficiency of methods available to extract biomass, especially from deep soil layers, and the possibility of altering microbial physiological status during extraction (Blagodatskaya and Kuzyakov, 2013a). We reduced this limitation by using a growth kinetics model and examined how depth and vegetation type influence microbial growth potentials. To our knowledge, this is the first study to assess microbial growth parameters along deep soil profiles. Overall, we did not observe significant differences in resource availability between vegetation types (see discussion 3 below), thus we primarily focus on the effects of soil depth on microbial parameters. We demonstrate that microbial communities in deep soil layers can grow relatively quickly in spite of significant evidence of dormancy (lower relative active microbial biomass), and that dormancy becomes more common as soil depth increases.

1. Maximum specific growth rate remains unchanged across 240 cm of soil profiles

In this study, maximum specific growth rate was relatively similar across the whole soil profile (0-240 cm; Fig. 5d), yielding an average of 0.33 ± 0.01 h^{-1}. Our estimation is comparable to those observed in other studies; maximum specific growth rate was 0.24-0.26 h^{-1} in agricultural topsoils (Blagodatskaya et al., 2014), 0.28-0.29 h^{-1} in soil suspension amended with acetate (Van De Werf and Verstraete, 1987), and 0.25-0.38 h^{-1} in an Ap horizon of loamy soil (Blagodatskaya et al., 2009). We acknowledge that the third assumption of the Panikov model, the whole microbial community behaves as a single entity (see Methods), is likely to be violated in the real world. This is because distinct microbial taxa often exhibit different physiological properties, including growth rate (Ho et al., 2018; Keiblinger et al., 2010; Koch et al., 2018; Morrissey et al., 2019, 2016). As such, we likely overestimated the whole community growth

rate, because relatively slowly growing microbes may have not responded to the yeast extract additions and thus we may have only captured the growth of fast growers.

Contrary to our first hypothesis that decreasing resource availability would reduce maximum specific growth rate across the soil profiles, there was no clear relationship between resource availability (C and N) and maximum specific growth rate (Table 1). High resource availability, especially for C, often triggers microbial transition from dormant to potentially active states (Blagodatskaya and Kuzyakov, 2013b; Kovárová-Kovar and Egli, 1998; Lennon and Jones, 2011). Yet, once microbes start growing in response to new resources, antecedent resource availability (i.e., resource availability before adding substrate) may be less relevant to achieving maximum growth rates. Instead, our observation suggests that intrinsic limits of microbial physiology may determine maximum growth potential (e.g., how fast intracellular enzymes catalyze biomolecule synthesis, how constitutively vs. inducibly enzymes are produced)(Adadi et al., 2012), or by the evolutionary history of individual taxa (Morrissey et al., 2019). Although they did not test for maximum specific growth rate, Stone et al. (2014) demonstrated that some extracellular enzymes' biomass-normalized activity does not change with soil depth despite decreasing resource availability along soil depth gradients. Invariant maximum specific growth rates across depth indicate that microbial communities maintain their growth potential regardless of the environmental conditions they inhabit.

Relatively invariant maximum specific growth rates across the whole soil profile have two ecological implications. First, the potential for microbial C transformation may be comparable between surface and deep soil layers. Most previous studies exploring microbial activity have focused on surface soils, assuming microbial activity is negligible in deeper soil layers. However, our data suggests microbial communities in deep soils can grow and transform soil C as much as surface microbes do. We acknowledge that we have only limited amount of data at 240 cm, but our data suggest that microbial communities at 240 cm exhibited similar maximum specific growth rate to those at surface soils (Fig.

5d). In addition, deep soil microbial communities at 210-240 cm were activated by C addition within 20 h (Fig. 5c) and increased their respiration rate (Fig. 4). Our results are in line with recent findings that microbial C transformations and associated CO_2 fluxes in deep soils (70 cm) are substantial (Min et al., 2020), microbial activities below 30 cm can be as high (Jones et al., 2018) or higher (Stone et al., 2014) than those at the surface. Also, a recent study revealed that root exudates from switchgrass enhanced microbial production of extracellular polymeric substances and soil C stability along 120 cm of soil profiles (Sher et al., 2020). Thus, given the similar maximum specific growth rates across depth profiles, potential microbial C transformation in deep soil layers can be relatively high.

Second, model representation of microbial growth across soil depth profiles can be simplified. A growing number of studies demonstrate that including microbial parameters improves model projections of the global C budget (Allison et al., 2010; Salazar-Villegas et al., 2016; Wang et al., 2015; Wieder et al., 2015, 2013). However, microbially-explicit models suffer from a lack of empirical knowledge on microbial parameters. Models require information on microbial biomass and biomass-specific rates, as process rates are often expressed as a product of the two (rates = biomass * biomass-specific rates). Our study provides evidence that models may treat microbial growth rate as a constant with soil depth, putting more emphasis on the accurate estimation of microbial biomass. Importantly, it will be critical to quantify active biomass because the active pool of microbes is a better predictor for biogeochemical processes than total biomass (Barnard et al., 2015; Couradeau et al., 2019; Salazar-Villegas et al., 2016; Salazar et al., 2019). In this study, we observed that total biomass was less sensitive to changes in soil depth than relative active biomass. For instance, total biomass decreased by four times while active biomass decreased by 134 times when soil depth changed from 0-20 cm to 210-240 cm (Fig. 5a,b). This suggests that if models employ total biomass, the errors associated with microbial process rates estimation would amplify with soil depth. Empiricists need to use approaches that allow them to

distinguish active from total biomass and better inform models of how active biomass would vary when environmental conditions change.

2. Active biomass decreases, and lag time increases with depth

As we hypothesized (second hypothesis), relative active biomass declined, and lag time increased with depth (Fig. 5b,c). Reductions in resource availability likely drove these changes in the relative active biomass and lag time (Table 1). Under conditions with relatively low available resources, microbes may enter dormancy (Lennon and Jones, 2011) or inhabit poorly connected colonies without quorum sensing (Mitri et al., 2016), likely increasing microbial lag time. Our results that deep soil layers contain low available resources (Fig. 2) and relatively low active microbes (Fig. 5b), and that lag time quickly drops at a low range of relative active biomass (S3) highlight that any increases in resource availability would disproportionately influence microbial communities in deep soil layers compared to those in topsoil layers. That is, microbial communities in deep soil layers might quickly shorten lag time if increases in resource availability were to drive increases in relative active biomass.

The relative active biomass in this study ranged from 0.02 (=2%) in 0-20 cm soils to 0.0001 (=0.01%) in 210-240 cm soils. Our estimates agree with other studies, where active biomass comprised less than 0.05% (Salazar et al., 2019), 0.1-2% (Blagodatskaya and Kuzyakov, 2013b), 0.2-0.6% (Blagodatskaya et al., 2009), or less than 3.5% (Bloem et al., 1992) of total biomass. These results imply that soil microbial growth is restricted even at topsoil layers with greatest resource availability, possibly due to lack of signal molecules (quorum sensing)(Atkinson and Williams, 2009) or unbalance in stoichiometry between resources and microbial biomass (Keiblinger et al., 2010; Sterner and Elser, 2002). Dormancy is much more common in soil compared to other systems such as freshwater (~50%) or marine water (~35%) (Lennon and Jones, 2011). This may be due to heterogeneity in soil's physicochemical properties and

425 highly fluctuating environmental conditions (Wallenstein and Hall, 2012; Wang et al., 2014). A great
426 proportion of dormancy in soils may help microbial communities cope with patchy and unpredictable
427 environmental variations and sustain their function over longer timescales (Lennon and Jones, 2011).

428 Many studies demonstrate that active biomass is closely associated with biogeochemical process rates
429 (Salazar-Villegas et al., 2016; Salazar et al., 2019), but we did not detect a clear relationship between
430 active biomass and basal respiration (basal respiration = 0.092 * active biomass + 0.365, R^2=0.12). One
431 explanation would be extremely low and highly variable basal respiration (0.45 ± 0.02 μg C-CO_2 g^{-1} dry
432 soil h^{-1}; S2) due to relatively low soil OC (Fig. 2a). In other studies, reported basal respiration is higher
433 than ours, at about 180-250 μg C-CO_2 g^{-1} dry soil h^{-1} at 0-15 cm of soil depth in a temperate forest
434 (Salazar-Villegas et al., 2016) and 3-4 μg C-CO_2 g^{-1} dry soil h^{-1} from the top 10 cm of a temperate
435 agricultural soil (Blagodatskaya et al., 2014). One study reports comparable values to our estimations at
436 0.18-0.24 μg C-CO_2 g^{-1} dry soil h^{-1} in mineral soils (Ritz and Wheatley, 1989). It is plausible that relatively
437 low and variable basal respiration may have decreased our ability to detect differences between
438 vegetation types or among depths, or a relationship between basal respiration and active biomass.

439

440 <u>3. Deeply rooted plants have little effect on microbial growth parameters</u>

441 Contrary to our third hypothesis, vegetation types did not influence microbial parameters in this study.
442 The discrepancy between the expectation and the observations is consistent with our finding that
443 switchgrass did not affect C and N availability (Fig. 2). Although the annual cropland was converted to
444 switchgrass more than a decade ago at our study site (Sekaran et al., 2019) and switchgrass developed a
445 deep rooting system (Fig. 1), the stocks of C and N, and ^{14}C values of bulk soil under switchgrass were
446 not distinguishable from those under soy (Fig. 2).

Several scenarios might explain the similar resource availability we observed between vegetation types. First, microbial respiration and priming may be greater under switchgrass than soy, canceling out likely higher plant C inputs from more, longer root growth. Soil C stock is a balance between inputs (litter, root exudates, root turnover) and outputs (respiration). If microbial respiration under switchgrass was enhanced (primed) due to greater plant C input, total soil C stocks may be similar between switchgrass and soy. Yet, similar basal respiration between the two vegetation types (S2) and similar ^{14}C values in bulk soil OC (Fig. 2b) suggest that this scenario is unlikely. Second, despite more, longer root growth under the switchgrass, the amount of root exudates may be comparable between switchgrass and soy. We did not directly quantify root exudates, but similar DOC concentrations between vegetation types (Fig.2c) suggest that this may be the case. Also, the main function may differ between deep and shallow roots. In a recent review (Lynch, 2019), deep roots are thought to collect water and nitrate, while shallow roots acquire nutrients such as phosphorus, calcium, and potassium. As nitrate is water-soluble, deep roots may not need to release root exudates as shallow roots do to mobilize nutrients. Third, the effects of vegetation and associated changes in the rooting depth on soil C stocks may be minimal in soils with high clay content and alkalinity. Recently, Slessarev et al. (2020b) demonstrated that C stocks were significantly higher under > 10-year-old switchgrass stands relative to annual crops in a low-nutrient sandy soil but found no consistent difference in the amount of C between deeply- and shallow-rooted plants in clayey soil. Soils at our study site were mostly clay loam (approximately 30% clay) with pH higher than 8.0 (S1). Thus, it is plausible that soil conditions may have influenced C accumulation along the soil profiles. Fourth, the annual cropland was fertilized in previous years and soy fixes N from the atmosphere. Contrary to switchgrass, the annual cropland is in rotation between soy and corn, and N fertilizer is used to enhance crop productivity. In addition, soy itself harbors N-fixing bacteria in roots. As such, it is plausible that residual N fertilizer applied in previous years and fixed N may persist to influence resource availability under soy. High dissolved N content under soy along the soil profiles

supports this argument (Fig. 2f). Taken together, the conversion from annual crops to switchgrass did not alter resource availability along soil depth profiles at our study site, which, in turn, marginally influenced microbial growth parameters between vegetation types.

CONCLUSIONS

Using a growth kinetics model, we estimated microbial growth parameters throughout soil depth profiles, a key knowledge gap for microbially-driven C dynamics models. While other studies have identified significant differences in profile-scale SOC inventories between switchgrass and shallow rooted conventional crops (Ferchaud et al., 2016; Liebig et al., 2005), in our study site, we did not observe enhanced soil C nor different microbial growth parameters under deep-rooted switchgrass compared to soy. The lack of a detectable plant-cover effect on both SOC stocks and microbial growth capacity may be a function of environmental factors, given that the response of bulk SOC pools to perennial cover can vary considerably as a function of soil properties, environmental conditions, and site history (Blanco-Canqui et al., 2005; Slessarev et al., 2020b). Depth profiles of microbial growth potential revealed increased dormancy rates at depth, but maximum growth potential was relatively similar across soil profiles. This suggests that a component of the microbial community at depth has the potential to rapidly exploit resources introduced by the deep root systems of perennial plants. Thus, to the extent that C inputs from deep root systems can increase SOC stocks, these deep SOC stocks are likely not immune from microbial transformation; rather, they might persist despite the presence of microbial consumers with a high capacity to assimilate fresh C.

493 **ACKNOWLEDGEMENTS**

494 We thank Drs. Sandeep Kumar and Udayakumar Sekaram at South Dakota State University for allowing
495 us to collect soil samples in their long-term experimental field site. This work was supported by
496 Lawrence Livermore National Laboratory's Lab Directed Research and Development program (#19-ERD-
497 010); the National Research Foundation of Korea (NRF) grant funded by the Korea government (MSIT;
498 NRF-2018R1A5A7025409); University of California Merced Chancellor's Fellowship to KM; University of
499 California Merced and Falasco Endowed Chair to AAB, and work at LLNL was conducted under the
500 auspices of DOE Contract DE-AC52- 07NA27344.

501

502

REFERENCES

Adadi, R., Volkmer, B., Milo, R., Heinemann, M., Shlomi, T., 2012. Prediction of microbial growth rate versus biomass yield by a metabolic network with kinetic parameters. PLoS Computational Biology 8. doi:10.1371/journal.pcbi.1002575

Allison, S.D., Czimczik, C.I., Treseder, K.K., 2008. Microbial activity and soil respiration under nitrogen addition in Alaskan boreal forest. Global Change Biology 14, 1156–1168. doi:10.1111/j.1365-2486.2008.01549.x

Allison, S.D., Wallenstein, M.D., Bradford, M.A., 2010. Soil-carbon response to warming dependent on microbial physiology. Nature Geoscience 3, 336–340. doi:10.1038/ngeo846

Anderson, J., Domsch, K., 1978. Mineralization of bacteria and fungi in chloroform-fumiaged soils. Soil Biology & Biochemistry 10, 207–213.

Atkinson, S., Williams, P., 2009. Quorum sensing and social networking in the microbial world. Journal of the Royal Society Interface 6, 959–978. doi:10.1098/rsif.2009.0203

Barnard, R.L., Osborne, C.A., Firestone, M.K., 2015. Changing precipitation pattern alters soil microbial community response to wet-up under a Mediterranean-type climate. ISME Journal 9, 946–957. doi:10.1038/ismej.2014.192

Berhe, A.A., Harden, J.W., Torn, M.S., Harte, J., 2008. Linking soil organic matter dynamics and erosion-induced terrestrial carbon sequestration at different landform positions. Journal of Geophysical Research 113, G04039. doi:10.1029/2008JG000751

Blagodatskaya, E., Blagodatsky, S., Anderson, T.H., Kuzyakov, Y., 2014. Microbial growth and carbon use efficiency in the rhizosphere and root-free soil. PLoS ONE 9. doi:10.1371/journal.pone.0093282

524 Blagodatskaya, E., Blagodatsky, S., Dorodnikov, M., Kuzyakov, Y., 2010. Elevated atmospheric CO2
525 increases microbial growth ratesin soil: results of three CO2 enrichment experiments. Global
526 Change Biology 16, 836–848.

527 Blagodatskaya, E., Blagodatsky, S.A., Anderson, T., Kuzyakov, Y., 2009. Contrasting effects of glucose,
528 living roots, and maize straw in microbial growth kinetics and substrate availability in sil. European
529 Journal of Soil Science 60, 186–197.

530 Blagodatskaya, E., Kuzyakov, Y., 2013a. Active microorganisms in soil: Critical review of estimation
531 criteria and approaches. Soil Biology and Biochemistry 67, 192–211.
532 doi:10.1016/j.soilbio.2013.08.024

533 Blagodatskaya, E., Kuzyakov, Y., 2013b. Active microorganisms in soil: Critical review of estimation
534 criteria and approaches. Soil Biology and Biochemistry 67, 192–211.
535 doi:10.1016/j.soilbio.2013.08.024

536 Blagodatsky, S.A., Blagodatskaya, E. V, Anderson, T., Weigel, H., 2006. Kinetics of the respiratory
537 response of the soil and rhizosphere microbial communities in a field experiment with an elevated
538 concentration of atmospheric CO2. Eurasian Soil Science 39, 290–297.
539 doi:10.1134/S1064229306030082

540 Blanco-Canqui, H., Lal, R., Lemus, R., 2005. Soil aggregate properties and organic carbon for switchgrass
541 and traditional agricultural systems in the southerneastern United States. Soil Science 170, 998–
542 1012.

543 Bloem, J., de Ruiter, P.C., Koopman, G.J., Lebbink, G., Brussaard, L., 1992. Microbial numbers and activity
544 in dried and rewetted arable soil under integrated and conventional management. Soil Biology and
545 Biochemistry 24, 655–665. doi:10.1016/0038-0717(92)90044-X

546 Brewer, T., Aronson, E., Arogyaswamy, K., Billings, S., Bothoff, J., Campbell, A., Dove, N., Fairbanks, D.,
547 Gallery, R., Hart, S., Kaye, J., King, G., Lohse, K., Maltz, M., O'Neil, C., Owens, S., Packman, A., Pett-
548 Ridge, J., Plante, A., Richter, D., Silver, W., Yang, W., Fierer, N., 2019. Ecological and genomic
549 attributes of novel bacterial taxa that thrive in subsurface soil horizons. MBio 10, mBio01318-19.

550 Contin, M., Todd, A., Brookes, P.C., 2001. The ATP concentration in the soil microbial biomass. Soil
551 Biology & Biochemistry 33, 701–704.

552 Couradeau, E., Sasse, J., Goudeau, D., Nath, N., Hazen, T.C., Bowen, B.P., Chakraborty, R., Malmstrom,
553 R.R., Northen, T.R., 2019. Probing the active fraction of soil microbiomes using BONCAT-FACS.
554 Nature Communications 10. doi:10.1038/s41467-019-10542-0

555 Ferchaud, F., Vitte, G., Mary, B., 2016. Changes in soil carbon stocks under perennial and annual
556 bioenergy crops. GCB Bioenergy 8, 290–306. doi:10.1111/gcbb.12249

557 Fierer, N., Allen, A.S., Schimel, J.P., Holden, P., 2003a. Controls on microbial CO2 production: A
558 comparison of surface and subsurface soil horizons. Global Change Biology 9, 1322–1332.
559 doi:10.1046/j.1365-2486.2003.00663.x

560 Fierer, N., Schimel, J.P., Holden, P.A., 2003b. Variations in microbial community composition through
561 two soil depth profiles. Soil Biology & Biochemistry 35, 167–176. doi:10.1016/S0038-
562 0717(02)00251-1

563 Flint, R.F., 1955. Pleistocene Geology of Eastern South Dakota. U.S. Geological Survey 173.
564 doi:10.3133/pp262

565 Gautier, D.L., 1986. Cretaceous shales from the western interior of North America: sulfur/carbon ratios
566 and sulfur-isotope composition. Geology 14, 225–228. doi:10.1130/0091-
567 7613(1986)14<225:CSFTWI>2.0.CO;2

568 Geyer, K., Kyker-Snowman, E., Grandy, A.S., Frey, S.D., 2016. Microbial carbon use efficiency : accounting
569 for population , community , and ecosystem-scale controls over the fate of metabolized organic
570 matter. Biogeochemistry 127, 173–188. doi:10.1007/s10533-016-0191-y

571 Graham, E.B., Knelman, J.E., Schindlbacher, A., Siciliano, S., Breulmann, M., Yannarell, A., Beman, J.M.,
572 Abell, G., Philippot, L., Prosser, J., Foulquier, A., Yuste, J.C., Glanville, H.C., Jones, D.L., Angel, R.,
573 Salminen, J., Newton, R.J., Bürgmann, H., Ingram, L.J., Hamer, U., Siljanen, H.M.P., Peltoniemi, K.,
574 Potthast, K., Bañeras, L., Hartmann, M., Banerjee, S., Yu, R.Q., Nogaro, G., Richter, A., Koranda, M.,
575 Castle, S.C., Goberna, M., Song, B., Chatterjee, A., Nunes, O.C., Lopes, A.R., Cao, Y., Kaisermann, A.,
576 Hallin, S., Strickland, M.S., Garcia-Pausas, J., Barba, J., Kang, H., Isobe, K., Papaspyrou, S., Pastorelli,
577 R., Lagomarsino, A., Lindström, E.S., Basiliko, N., Nemergut, D.R., 2016. Microbes as engines of
578 ecosystem function: When does community structure enhance predictions of ecosystem
579 processes? Frontiers in Microbiology 7, 1–10. doi:10.3389/fmicb.2016.00214

580 Hanson, C.A., Allison, S.D., Bradford, M.A., Wallenstein, M.D., Treseder, K.K., 2008. Fungal taxa target
581 different carbon sources in forest soil. Ecosystems 11, 1157–1167. doi:10.1007/s10021-008-9186-4

582 Harmon, T.C., Dierick, D., Trahan, N., Allen, M.F., Rundel, P.W., Oberbauer, S.F., Schwendenmann, L.,
583 Zelikova, T.J., 2015. Low-cost soil CO 2 efflux and point concentration sensing systems for
584 terrestrial ecology applications. Methods in Ecology and Evolution 6, 1358–1362.
585 doi:10.1111/2041-210X.12426

586 Hatzenpichler, R., Scheller, S., Tavormina, P.L., Babin, B.M., Tirrell, D.A., Orphan, V.J., 2014. In situ
587 visualization of newly synthesized proteins in environmental microbes using amino acid tagging
588 and click chemistry. Environmental Microbiology 16, 2568–2590. doi:10.1111/1462-2920.12436

589 He, S., Guo, L., Niu, M., Miao, F., Jiao, S., Hu, T., 2017. Ecological diversity and co- occurrence patterns of
590 bacterial community through soil profile in response to long-term switchgrass cultivation. Scientific

591 Reports 7, 3608. doi:10.1038/s41598-017-03778-7

592 He, Y., Yang, J., Zhuang, Q., Harden, J.W., McGuire, A.D., Liu, Y., Wang, G., Gu, L., 2015. Incorporating
593 microbial dormancy dynamics into soil decomposition models to improve quantification of soil
594 carbon dynamics of northern temperate forests. Journal of Geophysical Research: Biogeosciences
595 120, 2596–2611. doi:10.1002/2015JG003130

596 Ho, A., Lonardo, D.P. Di, Bodelier, P.L.E., 2018. Revisiting life strategy concepts in environmental
597 microbial ecology 1–14. doi:10.1093/femsec/fix006

598 IPCC, 2013. Climate change 2013: The physical science basis. Contribution of working group I to the Fifth
599 Assessment Report of the Intergovernmental Panel on Climate Change.

600 Jia, J., Cao, Z., Liu, C., Zhang, Z., Lin, L., Wang, Y., Haghipour, N., 2019. Climate warming alters subsoil but
601 not topsoil carbon dynamics in alpine grassland. Global Change Biology 25, 4383–4393.

602 Jobbágy, E.G., Jackson, R.B., 2000. The vertical distribution of soil organic carbon and its relation to
603 climate and vegetation. Ecological Applications 10, 423–436. doi:10.1890/1051-
604 0761(2000)010[0423:TVDOSO]2.0.CO;2

605 Jobbágy, E.G., Jackson, R.B., Biogeochemistry, S., Mar, N., 2001. The Distribution of Soil Nutrients with
606 Depth : Global Patterns and the Imprint of Plants Published by : Springer Stable URL :
607 http://www.jstor.org/stable/1469627 REFERENCES Linked references are available on JSTOR for
608 this article : You may need to log i. Biogeochemistry 53, 51–77.

609 Jones, D.L., Magthab, E.A., Gleeson, D.B., Hill, P.W., Sánchez-Rodríguez, A.R., Roberts, P., Ge, T., Murphy,
610 D. V., 2018. Microbial competition for nitrogen and carbon is as intense in the subsoil as in the
611 topsoil. Soil Biology and Biochemistry 117, 72–82. doi:10.1016/j.soilbio.2017.10.024

612 Kao-kniffin, J., Balser, T.C., 2008. Soil Fertility and the Impact of Exotic Invasion on Microbial

613 Communities in Hawaiian Forests 55–63. doi:10.1007/s00248-007-9323-1

614 Keiblinger, K.M., Hall, E.K., Wanek, W., Szukics, U., Hämmerle, I., Ellersdorfer, G., Böck, S., Strauss, J.,
615 Sterflinger, K., Richter, A., Zechmeister-Boltenstern, S., 2010. The effect of resource quantity and
616 resource stoichiometry on microbial carbon-use-efficiency. FEMS Microbiology Ecology 73, no-no.
617 doi:10.1111/j.1574-6941.2010.00912.x

618 Kennedy, M.J., Pevear, D.R., Hill, R.J., 2002. Mineral surface control of organic carbon in black shale.
619 Science 295, 657–660. doi:10.1126/science.1066611

620 Koch, B., McHugh, T., Hayer, M., Schwartz, E., Blazewicz, S., Dijkstra, P., van Gestel, N., Marks, J., Mau,
621 R., Morrisey, E., Pett-ridge, J., Hungate, B., 2018. Estimating taxon-specific population dynamics in
622 intact microbial communities. Ecosphere 9, DOI:10.1002/ecs2.2090.

623 Kögel-Knabner, I., Guggenberger, G., Kleber, M., Kandeler, E., Kalbitz, K., Scheu, S., Eusterhues, K.,
624 Leinweber, P., 2008. Organo-mineral associations in temperate soils : Integrating biology,
625 mineralogy, and organic matter chemistry. Journal of Plant Nutrition and Soil Science 171, 61–82.
626 doi:10.1002/jpln.200700048

627 Kohl, L., Morrill, P.L., Biesen, G. Van, Ziegler, S.E., 2015. Distinct fungal and bacterial d 13 C signatures as
628 potential drivers of increasing d 13 C of soil organic matter with depth 13–26. doi:10.1007/s10533-
629 015-0107-2

630 Kovárová-Kovar, K., Egli, T., 1998. Growth Kinetics of Suspended Microbial Cells: From Single-Substrate-
631 Controlled Growth to Mixed-Substrate Kinetics. Microbiology and Molecular Biology Reviews 62,
632 646–666. doi:10.1128/mmbr.62.3.646-666.1998

633 Lehmeier, C.A., Ballantyne IV, F., Min, K., Billings, S.A., 2016. Temperature-mediated changes in
634 microbial carbon use efficiency and 13C discrimination. Biogeosciences 13, 3319–3329.

635 doi:10.5194/bgd-12-17367-2015

636 Lennon, J.T., Jones, S.E., 2011. Microbial seed banks: The ecological and evolutionary implications of
637 dormancy. Nature Reviews Microbiology 9, 119–130. doi:10.1038/nrmicro2504

638 Li, J., Mau, R., Dijkstra, P., Koch, B., Schwartz, E., Purcell, A., Liu, X., Morrissey, E.M., Blazewicz, S.J., Pett-
639 Ridge, J., Stone, B., Hayer, M., Hungate, B., 2019. Predictive genomic traits for bacterial growth in
640 culture versus actual growth in soil. ISME Journal 13, 2162–2172.

641 Liebig, M., Johnson, H., Hanson, J., Frank, A., 2005. Soil carbon under switchgrass stands and cultivated
642 cropland. Biomass & Bioenergy 28, 347–354. doi:10.1016/j.biombioe.2004.11.004

643 Lynch, J.P., 2019. Root phenotypes for improved nutrient capture: an underexploited opportunity for
644 global agriculture. New Phytologist 223, 548–564. doi:10.1111/nph.15738

645 Manzoni, S., Taylor, P., Richter, A., Porporato, A., 2012. Environmental and stoichiometric controls on
646 microbial carbon-use efficiency in soils. New Phytologist 196, 79–91.

647 Martens, R., 1995. Current methods for measuring microbial biomass C in soil : Potentials and
648 limitations. Biology and Fertility of Soils 19, 87–99.

649 Martin, J., Sawyer, F., Fahrenbach, M., Tomhave, D., Schulz, L., 2004. Geologic map of South Dakota,
650 South Dakota Department of Environment & Natural Resources_Geological Survey.

651 McGowan, A., Nicolosa, R., Diop, H., Roozeboom, K., Rice, C., 2019. Soil organic carbon, aggregation,and
652 microbial community structure in annual and perennial biofuel crops. Agronomy Journal 111, 128–
653 142.

654 Min, K., Berhe, A.A., Khoi, C.M., van Asperen, H., Gillabel, J., Six, J., 2020. Differential effects of wetting
655 and drying on soil CO2 concentration and flux in near-surface vs. deep soil layers. Biogeochemistry

148, 255–269. doi:10.1007/s10533-020-00658-7

Min, K., Lehmeier, C.A., Ballantyne, F.I., Billings, S.A., 2016. Carbon availability modifies temperature responses of heterotrophic microbial respiration, carbon uptake affinity, and stable carbon isotope discrimination. Frontiers in Microbiology 7, doi: 10.3389/fmicb.2016.02083. doi:10.3389/fmicb.2016.02083

Mitchell, D.A., Von Meien, O.F., Krieger, N., Dalsenter, F.D.H., 2004. A review of recent developments in modeling of microbial growth kinetics and intraparticle phenomena in solid-state fermentation. Biochemical Engineering Journal 17, 15–26. doi:10.1016/S1369-703X(03)00120-7

Mitri, S., Clarke, E., Foster, K.R., 2016. Resource limitation drives spatial organization in microbial groups. ISME Journal 10, 1471–1482. doi:10.1038/ismej.2015.208

Morrissey, E.M., Dijkstra, P., Koch, B., Allen, K., Blazewicz, S., Hofmockel, K., Pett-Ridge, J., Hungate, B.A., 2019. Evolutionary history constrains microbial traits across environmental variation. Nature Ecology and Evolution 3, 1064–1069.

Morrissey, E.M., Mau, R.L., Schwartz, E., Caporaso, J.G., DIjkstra, P., Van Gestel, N., Koch, B.J., Liu, C.M., Hayer, M., McHugh, T.A., Marks, J.C., Price, L.B., Hungate, B.A., 2016. Phylogenetic organization of bacterial activity. ISME Journal 10, 2336–2340. doi:10.1038/ismej.2016.28

Panikov, N.S., 1995. Microbial growth kinetics. Springer.

Panikov, N.S., Sizova, M. V., 1996. A kinetic method for estimating the biomass of microbial functional groups in soil. Journal of Microbiological Methods 24, 219–230. doi:10.1016/0167-7012(95)00074-7

Paustian, K., Lehmann, J., Ogle, S., Reay, D., Robertson, G.P., Smith, P., 2016. Climate-smart soils. Nature 532, 49–57. doi:10.1038/nature17174

678 Pett-Ridge, J., Firestone, M.K., 2017. Rhizosphere Using stable isotopes to explore root-microbe-mineral
679 interactions in soil. Rhizosphere 1–10. doi:10.1016/j.rhisph.2017.04.016

680 Pries, C.E.H., Castanha, C., Porras, R.C., Torn, M.S., 2017. The whole-soil carbon flux in response to
681 warming. Science 1423, 1420–1423.

682 Ritz, K., Wheatley, R., 1989. Effects of water amendment on basal and substrate-induced respiration
683 rates of mineral soils. Biology and Fertility of Soils 8, 242–246.

684 Robertson, G.P., Coleman, D.C., Bledsoe, C., Sollins, P., 1999. Standard soil methods for long-term
685 ecological research. Oxford University Press, New York.

686 Rumpel, C., A, R.-R., Gonzalez-Perez, J., Arbelo, C., Chabbi, A., Nunan, N., Gonzalez-Vila, F., 2012.
687 Contrasting composition of free and mineral-bound organic matter in top- and subsoil horizons of
688 Andosols. Biology and Fertility of Soils 48, 401–411. doi:10.1007/s00374-011-0635-4

689 Rumpel, C., Kögel-Knabner, I., 2011. Deep soil organic matter — a key but poorly understood
690 component of terrestrial C cycle. Plant and Soil 338, 143–158. doi:10.1007/s11104-010-0391-5

691 Salazar-Villegas, A., Blagodatskaya, E., Dukes, J.S., 2016. Changes in the size of the active microbial pool
692 explain short-term soil respiratory responses to temperature and moisture. Frontiers in
693 Microbiology 7, 1–10. doi:10.3389/fmicb.2016.00524

694 Salazar, A., Lennon, J.T., Dukes, J.S., 2019. Microbial dormancy improves predictability of soil respiration
695 at the seasonal time scale. Biogeochemistry 144, 103–116. doi:10.1007/s10533-019-00574-5

696 Schmidt, M.W.I., Torn, M.S., Abiven, S., Dittmar, T., Guggenberger, G., Janssens, I. a., Kleber, M., Kögel-
697 Knabner, I., Lehmann, J., Manning, D. a. C., Nannipieri, P., Rasse, D.P., Weiner, S., Trumbore, S.E.,
698 2011. Persistence of soil organic matter as an ecosystem property. Nature 478, 49–56.
699 doi:10.1038/nature10386

700 Schwartz, E., Hayer, M., Hungate, B.A., Koch, B.J., Mchugh, T.A., Mercurio, W., Morrissey, E.M.,
701 Soldanova, K., 2016. Stable isotope probing with 18 O-water to investigate microbial growth and
702 death in environmental samples. Current Opinion in Biotechnology 41, 14–18.
703 doi:10.1016/j.copbio.2016.03.003

704 Sekaran, U., Mccoy, C., Kumar, S., Subramanian, S., 2019. Soil microbial community structure and
705 enzymatic activity responses to nitrogen management and landscape positions in switchgrass
706 (Panicum virgatum L.). Gloibal Change Biology: Bioenergy 11, 836–851. doi:10.1111/gcbb.12591

707 Sher, Y., Baker, N.R., Herman, D., Fossum, C., Hale, L., Zhang, X., Nuccio, E., Saha, M., Zhou, J., Pett-
708 Ridge, J., Firestone, M., 2020. Microbial extracellular polysaccharide production and aggregate
709 stability controlled by switchgrass (Panicum virgatum) root biomass and soil water potential. Soil
710 Biology and Biochemistry 143. doi:10.1016/j.soilbio.2020.107742

711 Singer, E., Wagner, M., Woyke, T., 2017. Capturing the genetic makeup of the active microbiome in situ.
712 ISME Journal 11, 1949–1963. doi:10.1038/ismej.2017.59

713 Slessarev, E.W., Lin, Y., Jiménez, B.Y., Homyak, P.M., Chadwick, O.A., D'Antonio, C.M., Schimel, J.P.,
714 2020a. Cellular and extracellular C contributions to respiration after wetting dry soil.
715 Biogeochemistry 147, 307–324. doi:10.1007/s10533-020-00645-y

716 Slessarev, E.W., Nuccio, E.E., McFarlane, K.J., Ramon, C.E., Saha, M., Firestone, M.K., Pett-Ridge, J.,
717 2020b. Quantifying the effects of switchgrass (Panicum virgatum) on deep organic C stocks using
718 natural abundance 14C in three marginal soils. GCB Bioenergy 1–14. doi:10.1111/gcbb.12729

719 Sterner, R.W., Elser, J., 2002. Ecological Stoichiometry: The biology of elements from molecules to the
720 biosphere. Princeton University Press.

721 Stone, M.M., Deforest, J.L., Plante, A.F., 2014. Changes in extracellular enzyme activity and microbial

community structure with soil depth at the Luquillo Critical Zone Observatory. Soil Biology and Biochemistry 75, 237–247. doi:10.1016/j.soilbio.2014.04.017

Stuiver, M., Polach, H., 1977. Discussion reporting of 14C data. Radiocarbon 19, 355–363.

Tomhave, D.W., Schulz, L.D., 2004. Bedrock Geologic Map Showing Configuration of the Bedrock Surface in South Dakota East of the Missouri River 100.

Trutko, S.M., Medentsev, A.G., Korobov, V.P., Akimenko, V.K., 1984. Cyanide-resistant respiration of bacteria and its relation to oversynthesis of metabolites. Mikrobiologiya 53, 21–27.

Van De Werf, H., Verstraete, W., 1987. Estimation of active soil microbial biomass by mathematical analysis of respiration curves: Development and verification of the model. Soil Biology and Biochemistry 19, 253–260. doi:10.1016/0038-0717(87)90006-X

Vance, E.D., Brookes, P.C., Jenkinson, D.S., 1987. An extraction method for measuring soil microbial biomass C. Soil Biology & Biochemistry 19, 703–707.

Vogel, J., Southon, J., Nelson, D., Brown, T., 1984. Performance of catalytically condensed carbon for use in accelerated mass spectrometry. Nuclear Instruments and Methods in Physics Research Section B 5, 289–293.

Wallenstein, M., Hall, E., 2012. A trait-based framework for predicting when and where microbial adaptation to climate change will affect ecosystem functioning. Biogeochemistry 109, 35–47. doi:10.1007/s10533-011-9641-8

Wang, G., Jagadamma, S., Mayes, M.A., Schadt, C.W., Megan Steinweg, J., Gu, L., Post, W.M., 2015. Microbial dormancy improves development and experimental validation of ecosystem model. ISME Journal 9, 226–237. doi:10.1038/ismej.2014.120

743 Wang, G., Mayes, M.A., Gu, L., Schadt, C.W., 2014. Representation of dormant and active microbial
744 dynamics for ecosystem modeling. PLoS ONE 9. doi:10.1371/journal.pone.0089252

745 Weishaar, J., Aiken, G., Bergamaschi, B., Fram, M., R, F., Mopper, K., 2003. Evaluation of specific
746 ultraviolet absorbance as an indicator of the chemical composition and reactivity of dissolved
747 organic carbon. Environmental Science & Technology 37, 4702–4708.

748 Wieder, W.R., Allison, S.D., Davidson, E.A., Georgiou, K., Hararuk, O., He, Y., Hopkins, F., Luo, Y., Smith,
749 M.J., Sulman, B., Todd-Brown, K., Wang, Y.P., Xia, J., Xu, X., 2015. Explicitly representing soil
750 microbial processes in Earth system models. Global Biogeochemical Cycles 29, 1782–1800.
751 doi:10.1002/2015GB005188

752 Wieder, W.R., Bonan, G.B., Allison, S.D., 2013. Global soil carbon projections are improved by modelling
753 microbial processes. Nature Climate Change 3, 1–4. doi:10.1038/nclimate1951

754 Wright, L., 2007. Historical perspective on how and why switchgrass was selected as a “model” high-
755 potential energy crop.

756 Wutzler, T., Blagodatsky, S.A., Blagodatskaya, E., Kuzyakov, Y., 2012. Soil microbial biomass and its
757 activity estimated by kinetic respiration analysis e Statistical guidelines. Soil Biology and
758 Biochemistry 45, 102–112. doi:10.1016/j.soilbio.2011.10.004

759 Zha, J., Zhuang, Q., 2020. Microbial dormancy and its impacts on northern temperate and boreal
760 terrestrial ecosystem carbon budget. Biogeosciences 17, 4591–4610. doi:10.5194/bg-17-4591-2020

761

762

FIGURE LEGENDS

Fig.1. Depth distribution of root biomass under switchgrass (blue) and soy (orange) in clay-loam agricultural fields in South Dakota.

Fig.2. Depth distribution of soil chemistry variables measured in switchgrass (blue) and soy (orange) clay-loam agricultural fields in South Dakota: (a) total organic carbon; (b) ^{14}C; (c) dissolved organic carbon; (d) specific UV absorbance of dissolved organic carbon (an index of aromaticity of dissolved organic carbon); (e) total nitrogen; (f) dissolved nitrogen. (n=3, error bars represent ± 1 standard error).

Fig.3. An example plot of soil microbial respiration from an agricultural soil incubated with (a) water only or (b) yeast extract plus water. The red dashed line indicates the time when water or yeast extract plus water was added.

Fig.4. Fitted model of microbial respiration from agricultural soil incubated with yeast extract for switchgrass (left) and soy (right) soils from 0 - 240 cm soil profiles. We used a growth kinetics model described in Panikov (1995). Different colors indicate different depth intervals. For visual simplicity, error bars have been omitted.

Fig.5. Depth distribution of microbial growth parameters estimated from a growth kinetics model in Panikov (1995), measured in switchgrass (blue) and soy (orange) soils incubated with yeast extract: (a) total microbial biomass before exponential growth; (b) relative active biomass before exponential growth, which varies between 0 and 1. If 0, all the biomass is dormant. If 1, all microbes actively grow and divide; (c) lag time, the response time of microbial community respiration rates to the additions of yeast extract; (d) maximum specific growth rate (μ_{max}), the maximum microbial growth potential per unit biomass per unit time (n=3, error bars represent ± 1 standard error).

785 **TABLES**

786 Table 1. Pearson's correlation coefficient between growth kinetics parameters and soil chemistry.

	OC	DOC	SUVA	N	Dissolved N
Total biomass	**0.47**	**0.46**	0.09	**0.49**	**0.41**
Relative active biomass	**0.63**	**0.75**	0.28	**0.60**	**0.76**
Lag time	**-0.70**	**-0.70**	-0.25	**-0.63**	**-0.59**
μ_{max}	0.31	0.22	0.12	0.26	0.15

787 Bold when $p < 0.05$

788

789 **SUPPLEMENTARY FIGURES**

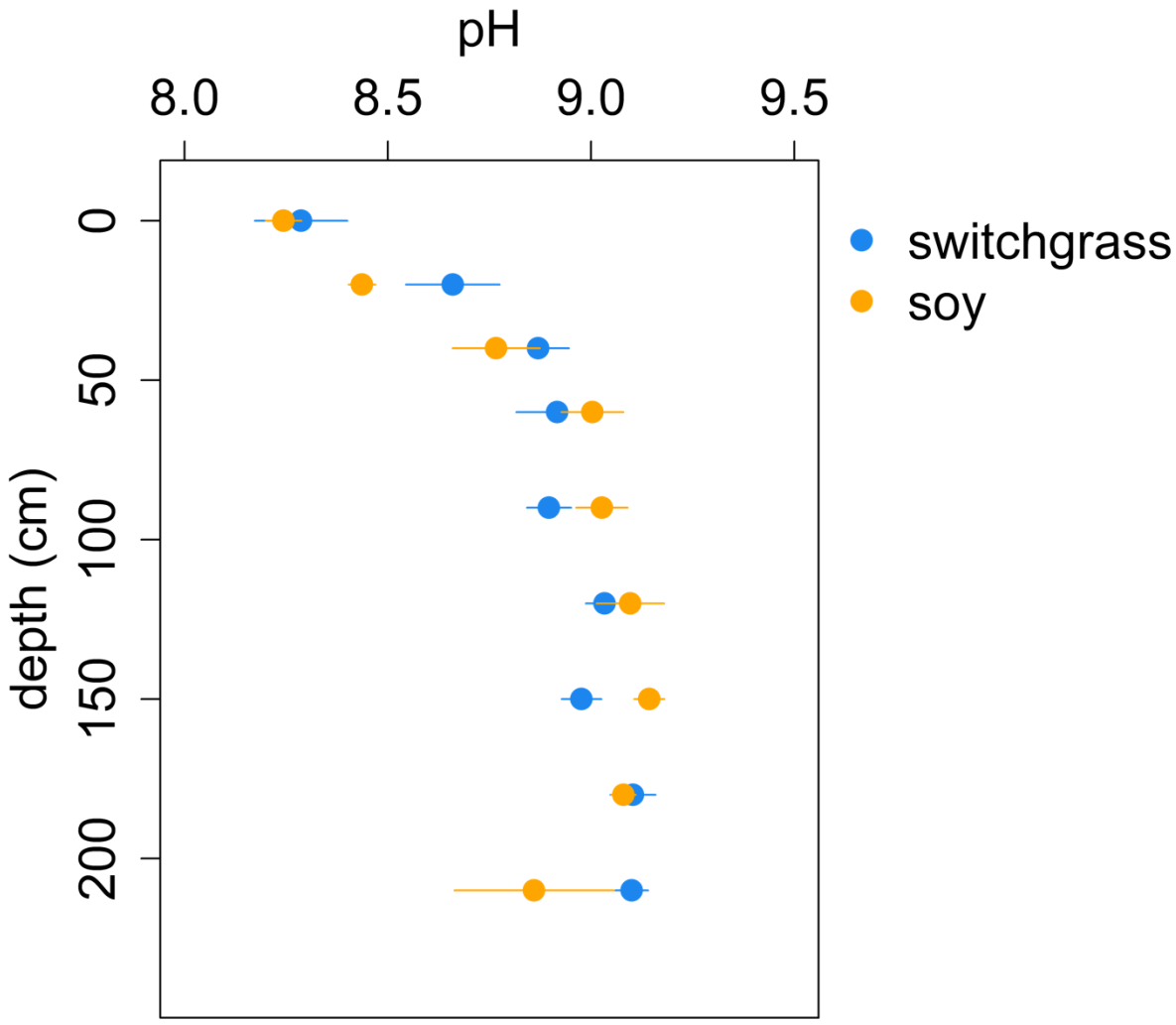

790

791 S1. Depth profile of soil pH for switchgrass (blue) and soy (orange) (n=3, error bars represent ± 1

792 standard error).

793

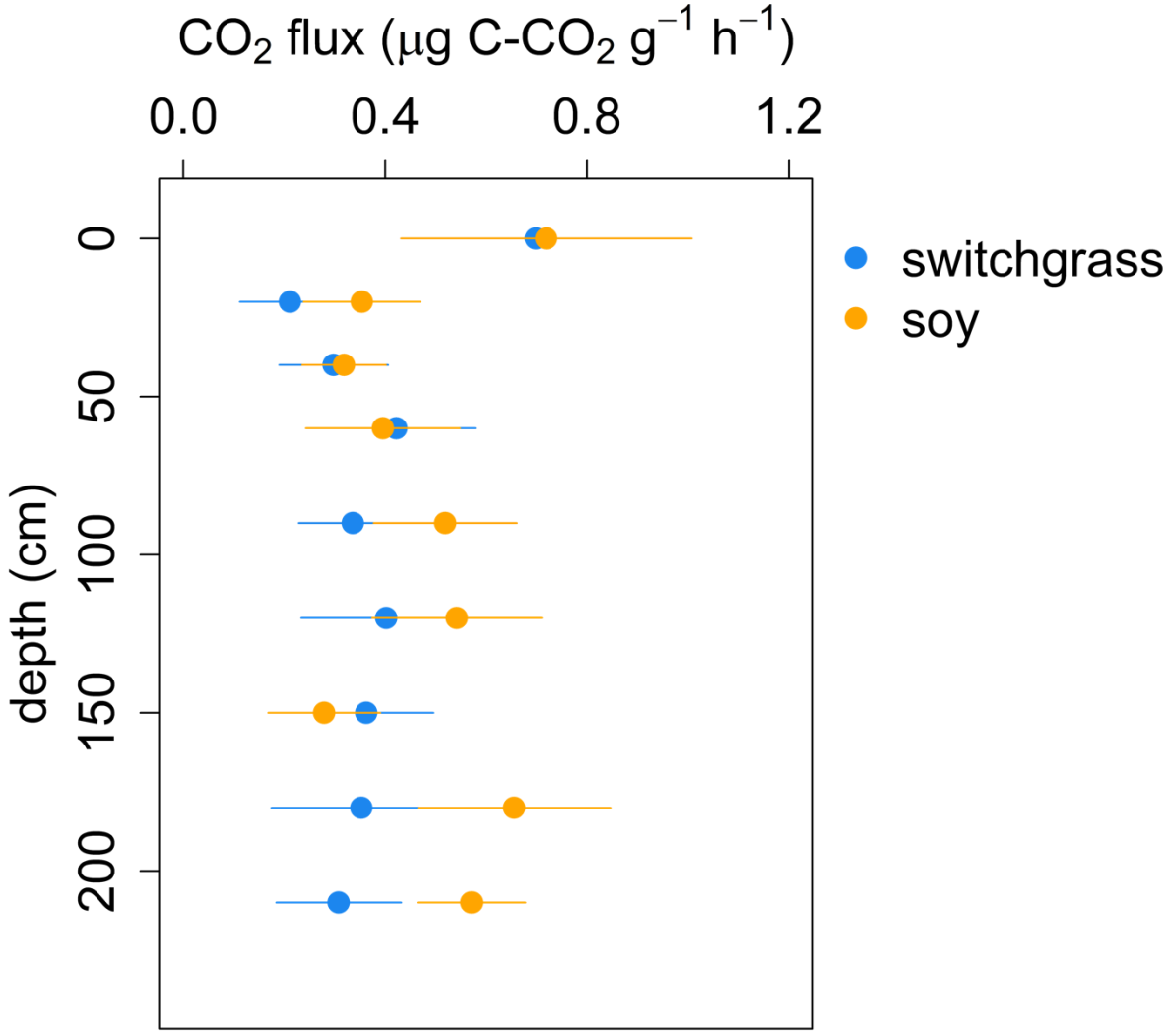

794

795 S2. Microbial basal respiration for switchgrass (blue) and soy (orange) soils collected along a 240 cm

796 depth profile from clay-loam agricultural fields in South Dakota (n=3, error bars represent ± 1 standard

797 error).

798

799

800

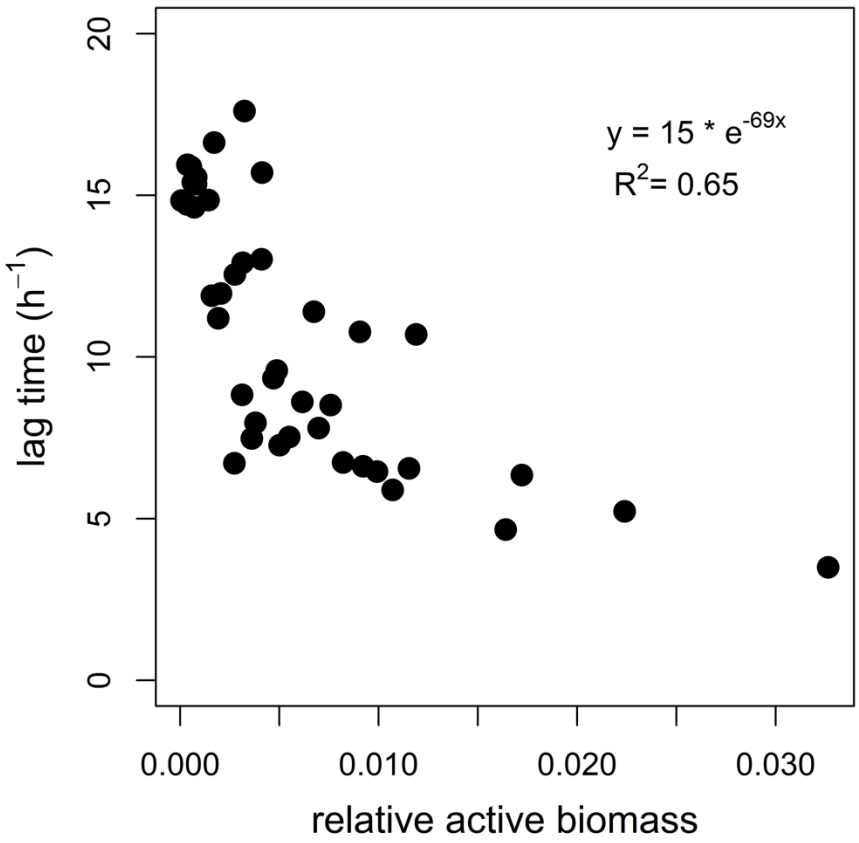

801

802 S3. Microbial lag time plotted against relative active biomass across vegetation type and depth.

803

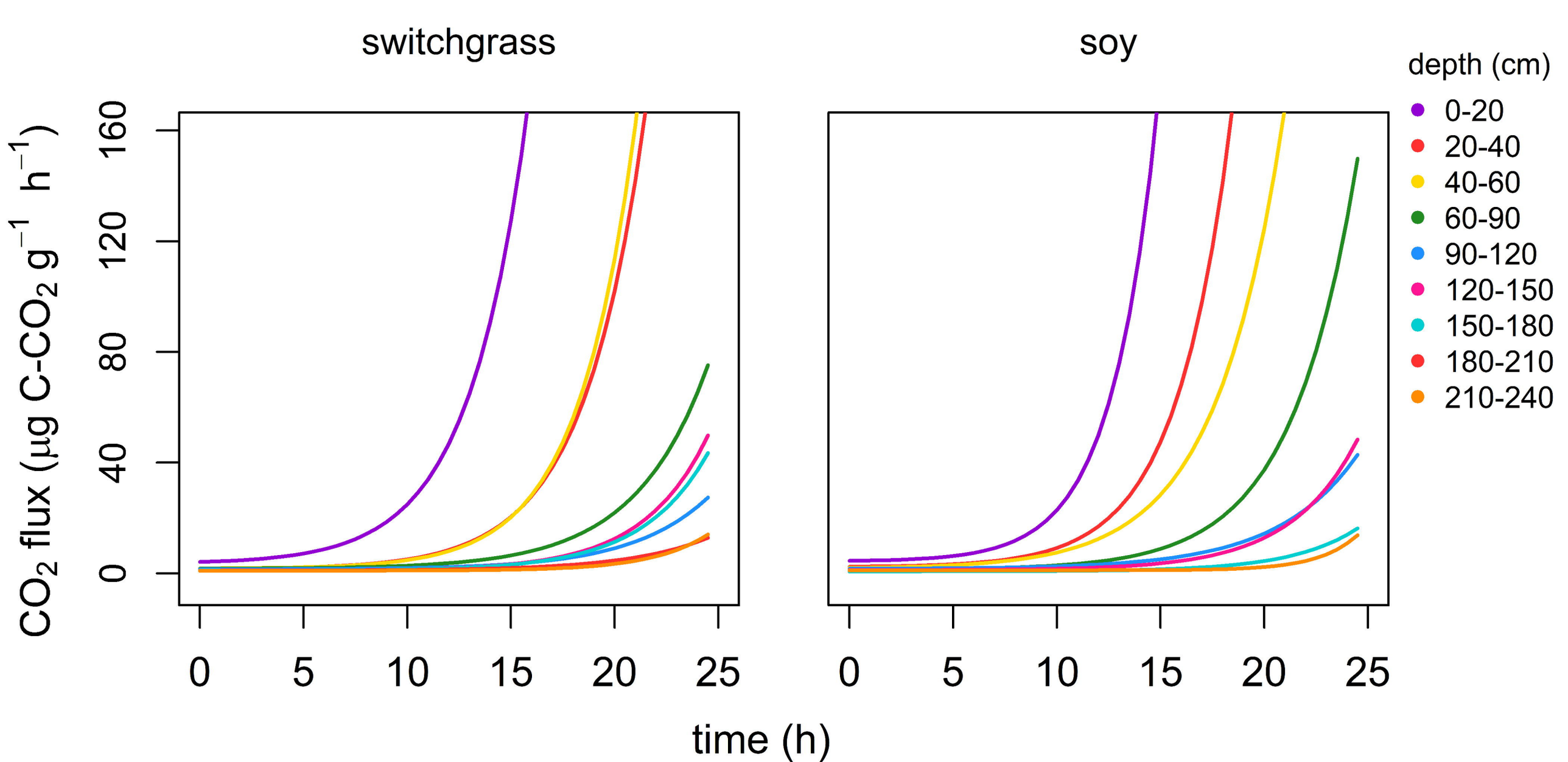
switchgrass
soy
depth (cm)
0-20
20-40
40-60
60-90
90-120
120-150
150-180
180-210
210-240
CO_2 flux (µg C-CO_2 g^{-1} h^{-1})
0
40
80
120
160
0
5
10
15
20
25
time (h)